gamma coincidences determined. Figure 4 shows a plot of $R=N_{\beta\gamma}/N_{\beta}$, the number of beta-gamma coincidences per recorded beta-particle as a function of the absorber thickness. From this graph it will be seen that, beyond a thickness of 0.12 cm Al (the range corresponding to beta-rays of 0.75-Mev energy) the curve is parallel to the axis. Below 0.12 cm the curve rises and there is an additional sharp break at 0.05 cm of aluminum, corresponding to a beta-particle energy of 0.47 Mev.

One would infer from Fig. 4 that there are at least three groups of electrons and that there are more gamma-rays associated with the lower energy groups than with the high energy ones. These experiments are in good agreement with the tentative energy level scheme which has been proposed as a result of the investigation of the beta- and gamma-ray spectrum in the magnetic lens.[8] One of the high intensity groups as proposed by these authors has an end point of 0.65 Mev. The first break in the $N_{\beta\gamma}/N_{\beta}$ curve comes at 0.75 Mev which is in reasonable agreement with the magnetic lens data. In addition, another group appears at 0.47 Mev, which is just at the position of the second break in the coincidence curve. Since the high energy part of the beta-ray spectrum, beyond 1 Mev contains very few electrons, it is difficult to measure coincidences in the neighborhood of the end point, 2.37 Mev. It cannot, therefore, be definitely inferred from these experiments that the highest energy group does or does not lead to the ground state of Te^{124}.

The work reported in this paper is essentially in agreement with that of MSG, with the exception that an additional low energy group has been found here. The work of MLM failed to detect any low energy groups, probably because the counters used at that time had walls which were too thick to transmit those groups. In conclusion, the authors would like to point out that, for an element with a decay scheme as complicated as that of Sb^{124}, it is not possible to work out a detailed disintegration scheme on the basis of coincidence experiments alone.

The authors wish to express their appreciation to the Office of Naval Research for their support of this work through Contract N6ori-48.

[8] See preceding paper by Kern, Zaffarano, and Mitchell.

PHYSICAL REVIEW VOLUME 73, NUMBER 10 MAY 15, 1948

X-Ray Yield Curves for $\gamma-n$ Reactions

G. C. BALDWIN AND G. S. KLAIBER*
General Electric Company, Schenectady, New York

(Received February 5, 1948)

Yield curves for the reactions $C^{12}(\gamma,n)C^{11}$ and $Cu^{63}(\gamma,n)Cu^{62}$ have been taken with x-rays up to 100 Mev. The induced radioactivity at each energy is plotted per unit x-ray intensity as measured by a r-meter thimble jacketed by $\frac{1}{8}$ in. of Pb. Both yield curves are similar to the photo-fission yield curves, the x-ray yield increasing to a maximum and then slowly decreasing as the x-ray energy is increased. With simple assumptions regarding the generation of ionizing secondaries in the Pb walls of the monitor and assumption of a constant intensity x-ray spectrum, these curves can be analyzed. The relative cross section is found to have a maximum at approximately 22 Mev for Cu^{62} and 30 Mev for C^{11}, decreasing to negligible values at high quantum energies. This decrease in cross section can be attributed to competition from multiple disintegrations. These reactions provide detectors sensitive only to part of the x-ray spectrum. Absorption curves have been taken in Pb using uranium photo-fission and in Cu and Pb using the $Cu^{63}(\gamma,n)Cu^{62}$ reaction as detectors. The resulting absorption coefficients compare favorably with theoretical values.

1. INTRODUCTION

INVESTIGATIONS which can be made with high energy quanta include measurements of cross section for photo-nuclear processes as a function of the energy of the absorbed quantum. In studying such processes with continuous x-rays generated by an electron accelerator, one

* Now at the University of Buffalo, Buffalo, New York.

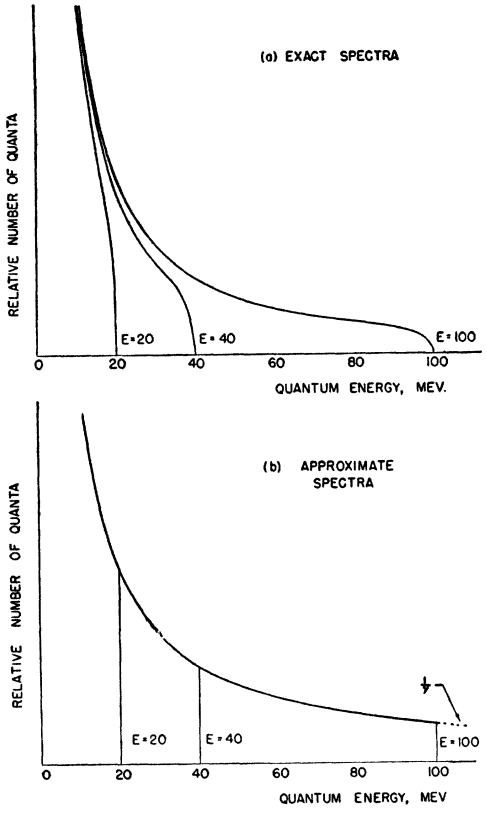

FIG. 1. Theoretical thin target bremsstrahlung spectra.

irradiates specimens of the substance concerned together with some sort of monitor at different x-ray energies, and obtains a "yield curve" in which the ratio of the yield of the process in question to the yield of the monitoring process is plotted against the x-ray energy; i.e., the maximum energy in the x-ray spectrum. To interpret such data, one must know the spectrum of the radiation and the response of the monitoring process to this spectrum at different x-ray energies.[1]

The curves in Fig. 1a are theoretical thin-target x-ray spectra given by the theory of bremsstrahlung.[2] The ordinates are relative numbers of quanta per unit energy interval, normalized to coincide at 10 Mev. The curves in Fig. 1b represent the distribution of quanta in "rectangular" spectra having equal intensity in every energy interval, the approximation used in cascade theory; even at these energies it will be seen by comparison with Fig. 1a that it is a good approximation. It will be noted that, were irradiations at various x-ray energies E so adjusted that all the respective spectra were normalized as in the figure, the difference between effects observed for neighboring values of E would be very nearly caused only by the action of those quanta whose energies, γ, lie between these values of E. To obtain the cross section as a function of γ from the yield curve, one differentiates the yield curve and divides it by the envelope of the spectrum curves.

In practice one cannot, of course, insure that the condition of normalization is satisfied.

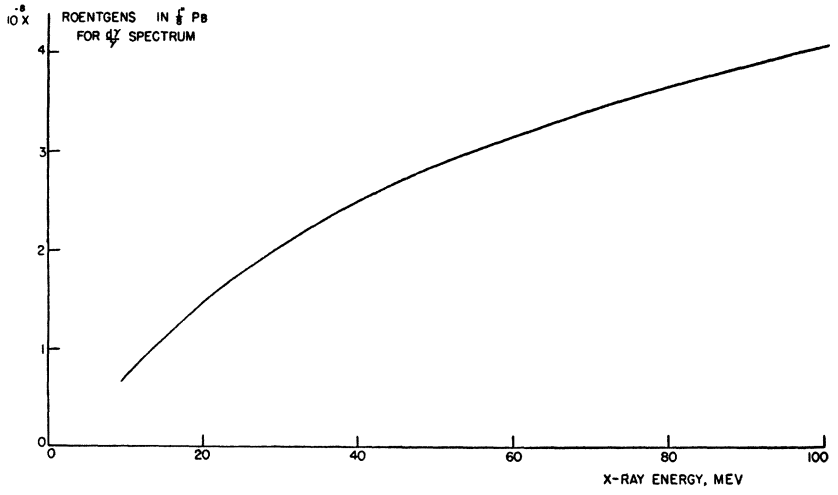

FIG. 2. Calculated sensitivity to the x-ray spectra of Fig. 1b of the monitor employed in these experiments.

[1] G. C. Baldwin and G. S. Klaiber, Phys. Rev. 71, 3 (1947).
[2] B. Rossi and K. Greisen, Rev. Mod. Phys. 13, 254 (1941).

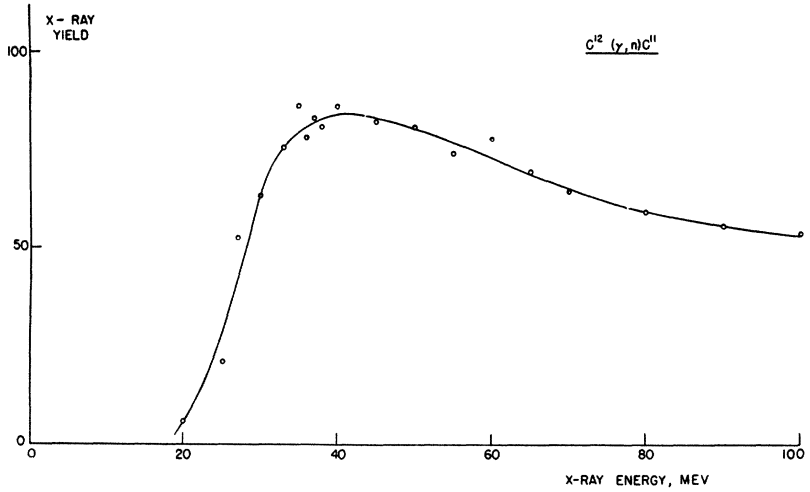

FIG. 3. X-ray yield of C^{11}.

Instead a monitor is employed. A Victoreen thimble r-meter surrounded by $\frac{1}{8}$-in. Pb forms a convenient if not perfect monitor. A more accurate monitor has been recently proposed but has not been tested experimentally.[3] The response of the former monitor to the approximate spectra of Fig. 1b as a function of E has been calculated,[1] assuming it to be due to ionization by electron secondaries generated by pair production, scattering and photo-effect, proceeding mainly in the forward direction and not generating an appreciable number of cascade processes in the $\frac{1}{8}$-in. Pb wall of the monitor. This response is shown in Fig. 2. If the experimentally obtained yield curve is multiplied by the monitor response curve, $r(E)$, the product is the yield curve for a normalized family of spectra, and can be analyzed by differentiation and division by the spectrum envelope, $1/\gamma$, as explained above.

We have previously reported measurements of the x-ray yields of fission of uranium and thorium, which indicated that the photo-fission cross section rises to a maximum at approximately 16 Mev, decreasing at higher energies to become negligibly small above 30 Mev. This effect was ascribed to the competition of other types of photo-disintegration[4] that can occur at higher energies. It has seemed worthwhile to

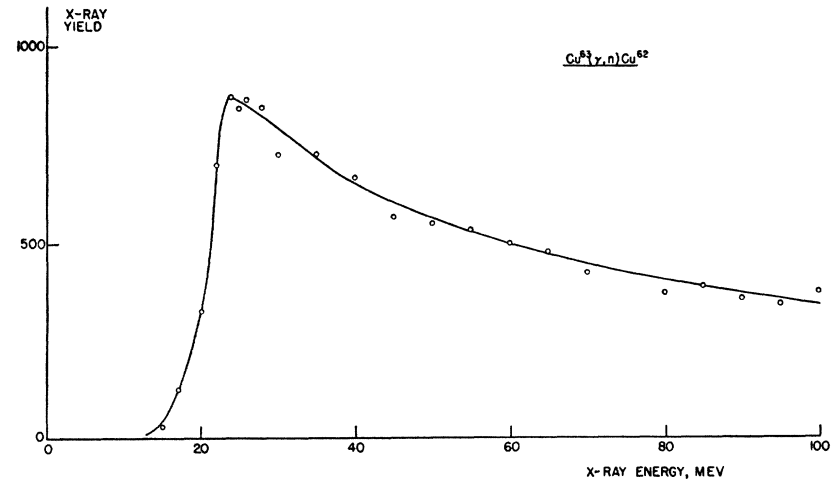

FIG. 4. X-ray yield of Cu^{62}.

[3] M. Lax, Phys. Rev. **72**, 61 (1947).
[4] G. C. Baldwin and G. S. Klaiber, Phys. Rev. **70**, 259 (1946).

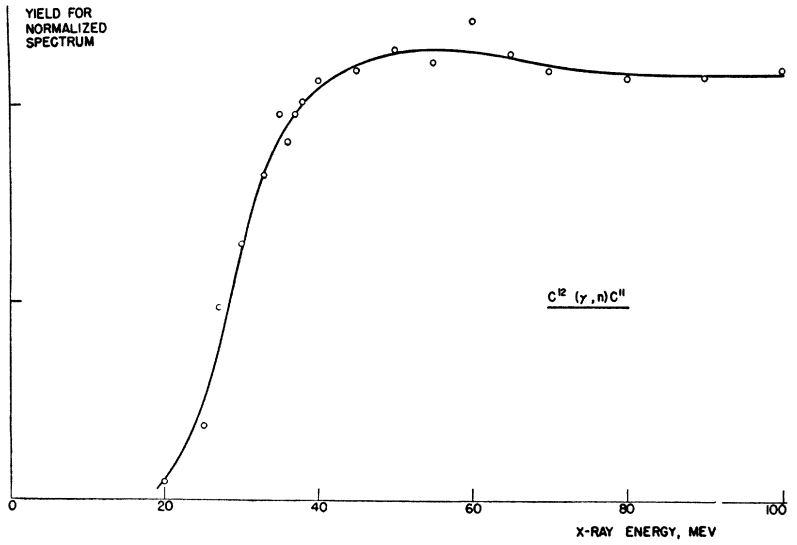

FIG. 5. Product of the curves of Figs. 2 and 3.

extend these measurements to other processes. It was also desired to obtain confirmatory evidence to support the validity of the method of analysis used and conclusions reached.

2. (γ,n) YIELD MEASUREMENTS

The reactions investigated were $C^{12}(\gamma,n)C^{11}$ and $Cu^{63}(\gamma,n)Cu^{62}$. The carbon samples were polythene sheets, 2 in. square by 0.03 in. thick; the copper foils 2 in. square by 0.003 in. thick. A special clamp held each sample for irradiation at a reproducible position 67 in. from the target in the center of the x-ray beam from the 100-Mev betatron, the lead-jacketed r-meter thimble being clamped immediately behind the sample. Decay curves were first taken which established that no activity other than C^{11} or Cu^{62} gave appreciable contribution to the measured activity for the irradiation time of 20 minutes. The samples were then irradiated at various x-ray energies, transferred to a G-M counter and counted in a standard position for two half-lives. Corrections were made for background and for losses at fast rates of counting, the latter taking account of the fourfold variation in counting rate over the measurement period. The resulting yield curves for C^{11} and Cu^{62} are shown in Figs. 3 and 4. The ordinates are ratios of the saturation initial activity in counts per minute per gram of sample to the number of roentgens per minute registered

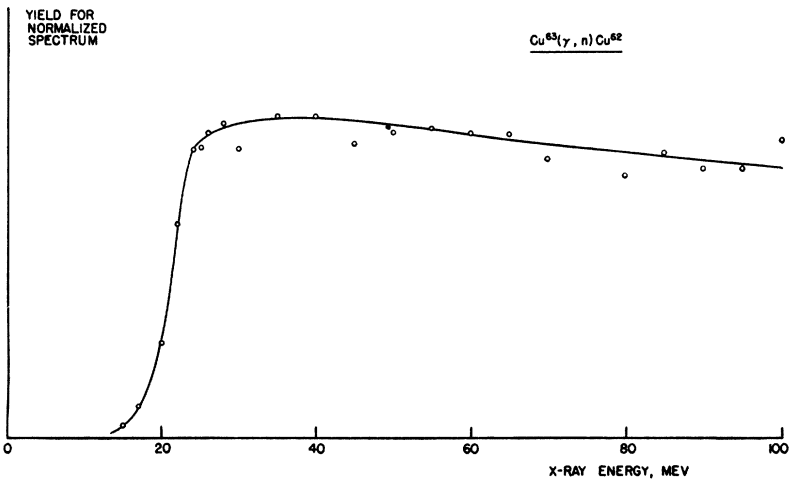

FIG. 6. Product of the curves of Figs. 2 and 4.

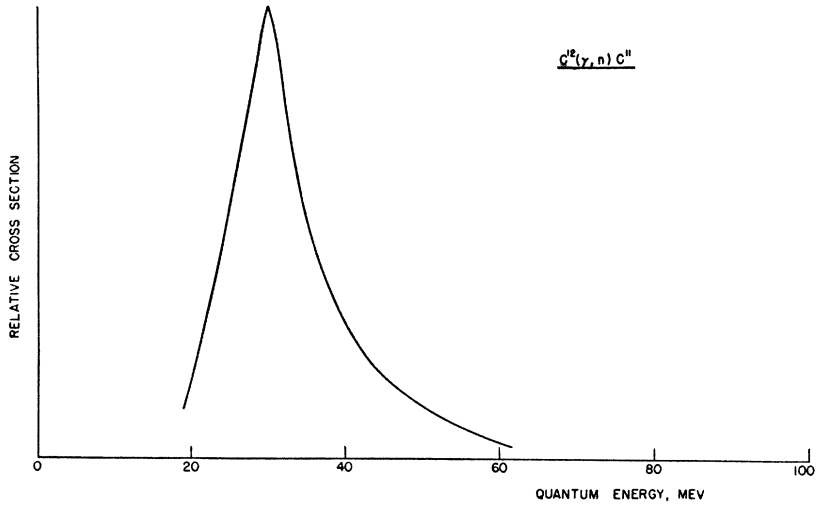

FIG. 7. Approximate cross section for $C^{12}(\gamma,n)C^{11}$, arbitrary units.

by the monitor. Both curves show the same behavior as the x-ray yield for photo-fission—a steep rise from threshold to a maximum, followed by a gradual decrease in yield at higher x-ray energies. The maxima occur at 40 Mev for $C^{12}(\gamma,n)$ and at 24 Mev for $Cu^{63}(\gamma,n)$. The maximum x-ray yield for $U(\gamma,f)$ was at 18 Mev, for $Th(\gamma,f)$ at 20 Mev.[1]

The respective yield curves for production by a normalized family of spectra, obtained by multiplying each yield curve by the function in Fig. 2 are shown in Figs. 5 and 6. From these as in the case of fission, it is apparent that the decreasing x-ray yield at energies above that corresponding to the maximum is in both cases probably due to rising sensitivity of the monitor and that quanta of high energies do not induce the reaction.[5]

The approximate cross sections, shown in Fig. 7 and Fig. 8, have maxima near 30 Mev for C^{11}, 22 Mev for Cu^{62}.

This behavior of the (γ,n) cross section is to be expected as a result of the competition of multiple disintegration processes once these become energetically possible. In Table I are given several photo-nuclear reactions on C^{12} together with their thresholds calculated from mass and

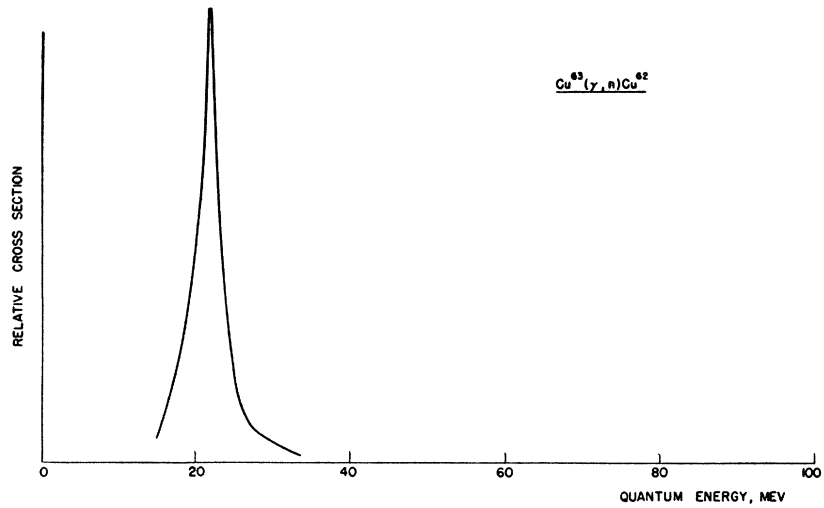

FIG. 8. Approximate cross section for $Cu^{63}(\gamma,n)Cu^{62}$, arbitrary units.

[5] The slight negative slope still present in these curves probably indicates that the true monitor sensitivity rises slightly faster with x-ray energy than the function in Fig. 2. This is probably owing to cascade processes in the lead wall of the monitor, neglected in the calculation; the error is not serious.

beta-decay energies. It is evident that above 27 Mev many alternative disintegration processes can compete with the single-neutron process. The latter, involving a relatively improbable concentration of the entire excitation energy on a single particle or on the latter and a gamma-ray, will be relatively rare.

That "star" processes, similar to the last entry of Table I, occur at fairly low photon energies is evidenced by the star shown in Fig. 9 produced in a 12-in. air-filled cloud chamber with 100-Mev x-rays. This may be a carbon disintegration of this type, but it is believed more likely that it is a disintegration of N^{14} into three alphas, a proton, and a neutron. On this assumption the data of Table II are deduced from measurements

TABLE I. Photo-nuclear thresholds for C^{12}.

Reaction	Threshold (Mev)
$C^{12}(\gamma,p)B^{11}$	15.9
$C^{12}(\gamma,n)C^{11}$	18.6
$C^{12}(\gamma,2p)Be^{10}$	27.0
$C^{12}(\gamma,pn)B^{10}$	27.2
$C^{12}(\gamma,2n)C^{10}$	32.3
$C^{12}(\gamma,2pn)Be^{9}$	33.6
$C^{12}\xrightarrow{\gamma}2\alpha+2p+2n$	35.4

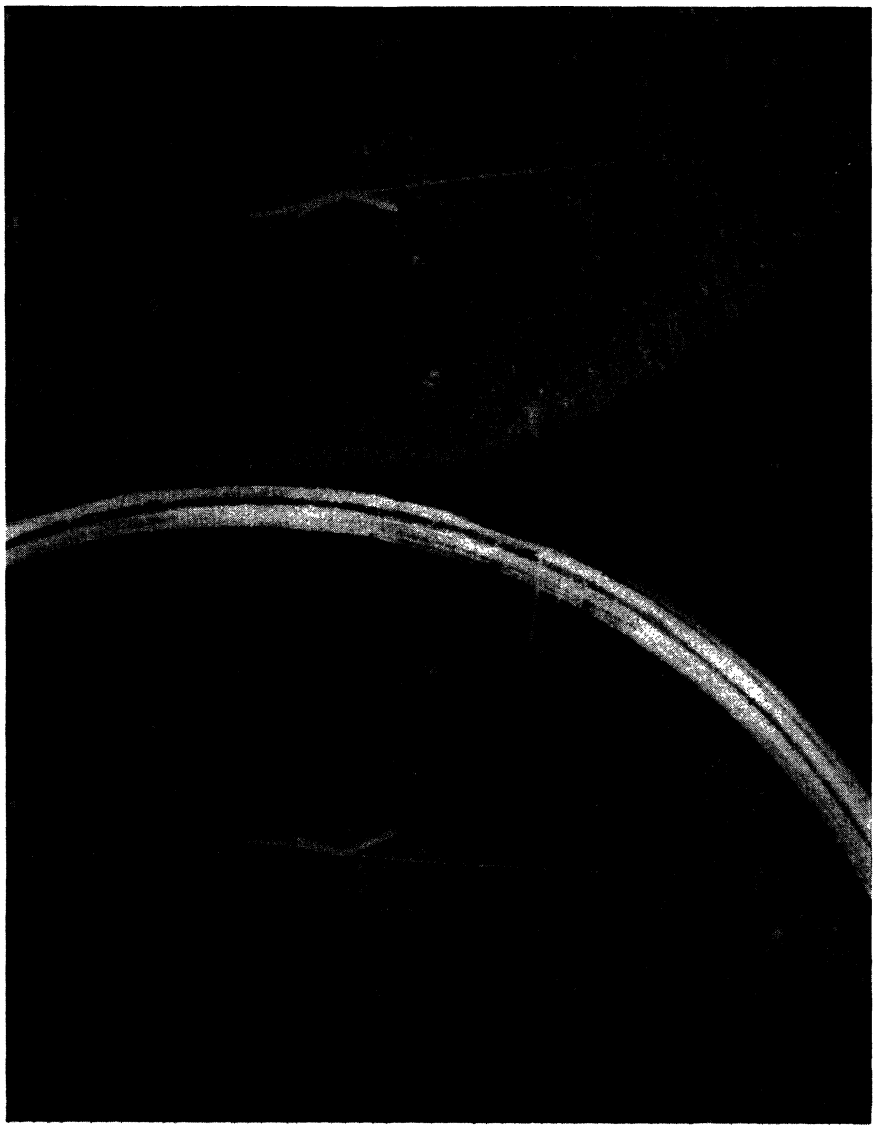

FIG. 9. Tracks of a nuclear evaporation photographed in a 12-in. air-filled cloud chamber; the analysis is given in Table II. The x-ray beam enters from below in the direct (lower) image.

TABLE II. Analysis of the "star" of Fig. 9. Reaction: $_7N^{14}+\gamma\rightarrow{}_1H^1+3\,{}_2He^4+{}_0n^1$.

Particle	$_1H^1$	$_2He^4$	$_2He^4$	$_2He^4$	$_0n^1$
Data	$H\rho=4.3\times10^5$	$R=2.35$ cm.	$R=1.25$ cm.	$R=1.35$ cm.	
Energy, Mev	9.4	3.8	2.4	2.5	2.5
Angle to beam	96°	82°	75°	68°	145°
Azimuth	262°	76°	76°	248°	260°

Calculated threshold = 20 Mev
Total kinetic energy of products = 21 Mev
Energy of incident quantum = 41 Mev

of range or curvature and directions of emission. All of the particles are of low energy, the 40-Mev excitation dividing about equally between binding energy and kinetic energy.

The conclusion that the (γ,n) cross sections become small at high energies is consistent with the observations of Perlman and Friedlander on relative yields at 50 and 100 Mev of several (γ,n) reactions.[6]

3. ABSORPTION MEASUREMENTS

Additional support for this conclusion is found when the absorption of quanta is measured using the photo-nuclear reaction as a detection process.

In Fig. 10 is shown an absorption curve in which the detection process is uranium photo-fission. The ionization chamber[1] was placed in the 100-Mev x-ray beam and fission counts taken with the beam passing through absorbing slabs of lead to reach the chamber. The activity induced in a Cu foil ahead of the Pb was used to monitor each run. The exponentials drawn for comparison have slopes corresponding to theoretical absorption coefficients in Pb for quanta of the energies indicated.[7]

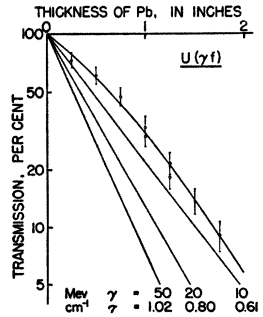

FIG. 10. Absorption of fission-producing component of 100-Mev x-rays.

Figures 11 and 12 present absorption curves taken in Cu and Pb, respectively, with 100-Mev x-rays using the $Cu^{63}(\gamma,n)Cu^{62}$ reaction as detector. A pair of Cu foils, 2 in. square by 0.003 in. thick were placed, one just ahead of a 4-in. $\times$4-in. $\times$10-in. block of the absorbing material and the other at a variable depth, x, in the block. These were irradiated simultaneously, then transferred to G-M counters. Each foil's activity was counted for a standard period of one half-life, then the samples were interchanged and the count repeated. From ratios of the three possible products by pairs of the recorded counts was obtained the ratio of sample activities, ratio of counter efficiencies, and ratio of average activity of either sample in the first to that in the second counting period. The latter two data, being constants, provided checks on each run to insure against mistakes or other errors.[8]

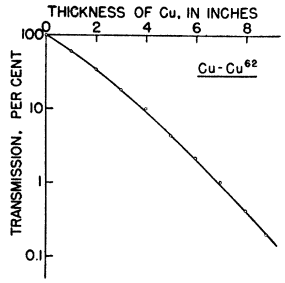

FIG. 11. Absorption in copper of that component of 100-Mev x-radiation which produces the reaction $Cu^{63}\rightarrow Cu^{62}$.

[6] M. L. Perlman and G. Friedlander, Phys. Rev. **72**, 1272 (1947).

[7] W. Heitler, *The Quantum Theory of Radiation* (Oxford University Press, New York, 1944), second edition, Chapter V.

[8] It will be noted from Fig. 12 that deep in the absorber a constant background is present, arising from the reaction $Cu^{63}(n,2n)Cu^{62}$ induced by photo-neutrons in the Pb absorbing block. Since this background is less than 0.1 percent of the Cu^{62} activity observed at the surface of the

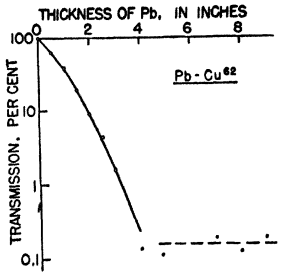

FIG. 12. Absorption in lead of that component of 100-Mev x-radiation which produces the reaction $Cu^{63} \rightarrow Cu^{62}$.

The results are summarized in Fig. 12, which gives the absorption coefficient as a function of depth in the absorbing block, together with theoretical absorption coefficients for radiation of various energies.[7] The experimental curves are, of course, not exponential because:

1. Cascade shower processes build up quanta in the lower energy region of the spectrum.

2. Compton scattering processes in which the energy of the scattered photon remains above the Cu^{62} threshold do not appear as absorption, and, in fact, may appear as a generation of quanta to a detector sensitive only to the lower energy portion of the x-ray spectrum. This effect becomes less important as the spectrum is degraded by passing through increasing thicknesses of absorber.

absorber, it is legitimate to consider the Cu^{62} yield in Fig. 4 to be induced by quanta alone. That this is also true of the photo-fission yields reported in reference 1 is indicated by observations that the fission yield is unaffected by changing the surrounding material from aluminum and brass to graphite and polystyrene, that the fission yield is proportional to the thickness for small thicknesses of the uranium target, that the fission-producing radiation is confined to a beam of 3° half-angle coaxial with the x-ray beam and is absorbed like gamma-radiation (Fig. 10).

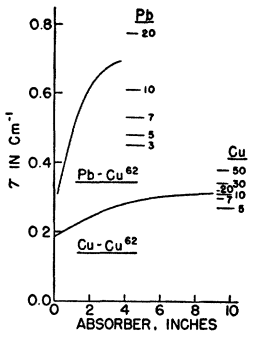

FIG. 13. Summary of absorption data of Figs. 11 and 12. Theoretical absorption coefficients of Cu and Pb are also given for various quantum energies in Mev.

3. The detecting process does not respond only to a single quantum energy but to a band of energies, within which the absorption coefficient varies by an appreciable extent.

Asymptotically, however, the absorption curve should approach an exponential of slope corresponding to the most penetrating component within the energy region in which the detector responds. It will be evident from Fig. 12 that this limiting value of the absorption coefficient compares favorably with that expected theoretically for quanta in the energy region where, according to the analysis of the x-ray yield curves, the detecting reaction has an appreciable cross section.

4. ACKNOWLEDGMENT

We wish to express our appreciation to Mr. C. E. Pickert for his assistance in taking the experimental data and the calculations, to Mr. R. H. Groncznack for assistance with the cloud chamber, and to the operating staff of the 100-Mev betatron.

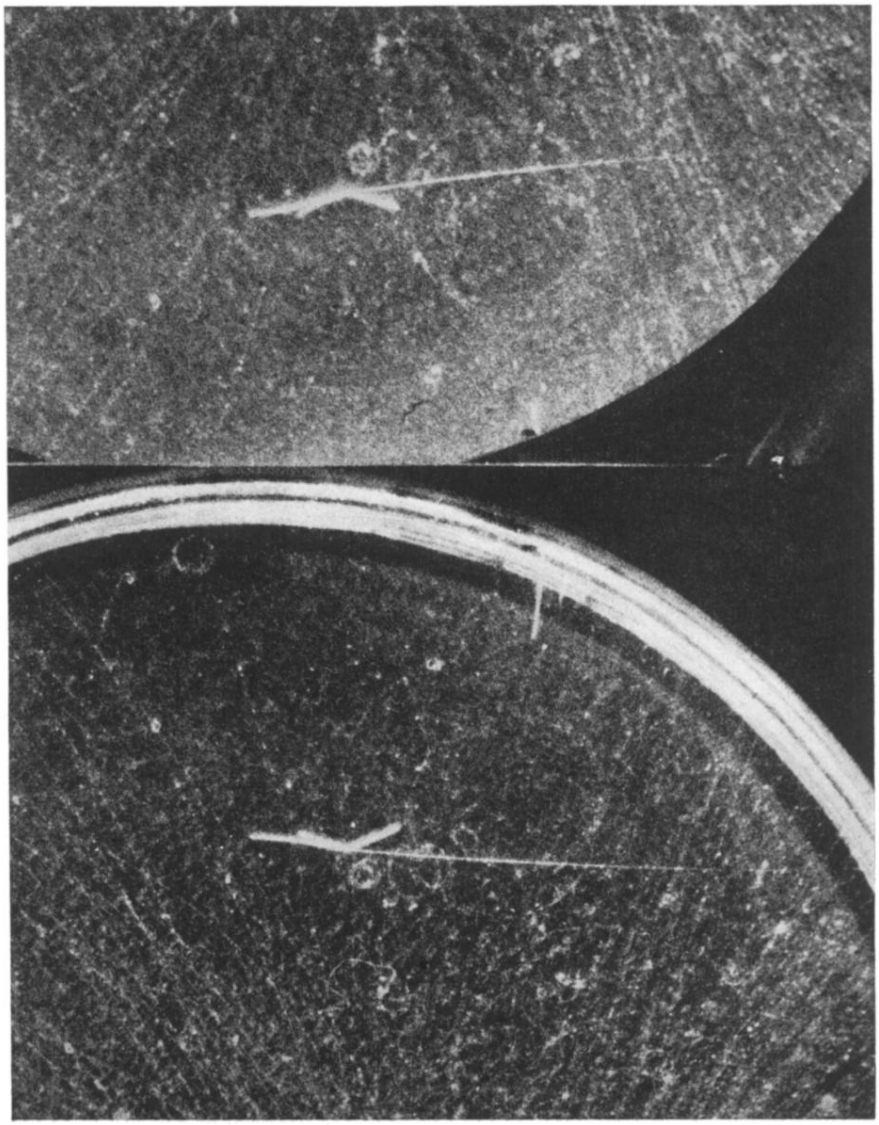

FIG. 9. Tracks of a nuclear evaporation photographed in a 12-in. air-filled cloud chamber; the analysis is given in Table II. The x-ray beam enters from below in the direct (lower) image.